Agrociencia

NUMERICAL SIMULATION AND OPTIMIZATION OF THE POTATO HARVESTER DIGGING SHOVEL IN HILLY AREAS

Qixin **Wang**[1], Chunyan **Kong**[1*], Mingkun **Yang**[1], Yang **Li**[1], Yi **Liao**[1]

[1] Xihua University. School of Mechanical Engineering. Chengdu, China. 610039.
*Corresponding author: kongcy@mail.xhu.edu.cn

Citation: Wang Q, Kong C, Yang M, Li Y, Liao Y. 2024. Numerical simulation and optimization of the potato harvester digging shovel in hilly areas. **Agrociencia.** https://doi.org/ 10.47163/agrociencia.v58i6.3144

Editor in Chief:
Dr. Fernando C. Gómez Merino

Received: January 17, 2024.
Approved: September 12, 2024.
Published in Agrociencia: September 23, 2024.

ABSTRACT

The shovel face inclination angle is a crucial parameter of the potato harvester digging shovel. Currently, there is limited research on the relationship between the inclination angles of curved digging shovel surfaces. The purpose of this study was to investigate the impact of the shovel face inclination angle on its soil crushing capacity in hilly terrain. A simulation model for the contact between the digging shovel and the soil was developed. The digging process of the shovel was simulated and analyzed under different shovel face inclination angles (α_2). The analysis included comparisons of stress, Plastic Equivalent Strain (PEEQ), and energy. The results show that the larger the angle, the stronger its soil crushing ability; however, if the angle difference is too large, the phenomenon of soil flipping back occurs. When α_2 = 16–17 °, the shovel length becomes excessive. When α_2 = 18 °, the stress is too small. When α_2 = 19 °, the energy is too large, and when α_2 = 23–24 °, the PEEQ is too small. Therefore, the optimal shovel face inclination angle α_2 is between 20 and 22 °, with fixed angles α_1 = 15 ° and α_3 = 13 °.

Keywords: shovel face inclination angle, structure optimization.

INTRODUCTION

The digging shovel is an essential component of a potato harvester. They are classified into flat shovels, curved shovels, and biomimetic shovels (Wei *et al*., 2013). The digging shovel is comprised of several parameters, including shovel length, blade opening angle, shovel face inclination angle, and shovel width. The inclination angle is one of the most important parameters. When the potato harvester is operating, an excessively large shovel face inclination angle can increase resistance and cause the potato soil mixture to flip back. Conversely, a too-small angle can result in an elongated shovel length and soil clogging.

The shovel face inclination angle affects the digging shovel's soil crushing capacity, soil penetration ability, and lifting capability. Flat shovels and curved shovels are two common types of digging shovels; however, flat shovels do not consider the digging shovel's soil crushing capacity, whereas curved shovels consider not only the crushing capacity but also the soil penetration and loosening ability. This facilitates the subsequent separation of the potato mixture and ensures the safety of the digging shovel.

Wei *et al*. (2024) addressed the issue of the digging shovel of the potato harvester failing to achieve early soil leakage, resulting in significant digging resistance. Drawing inspiration from the unique advantages of a wild boar's snout, they designed a biomimetic digging shovel. Wang *et al*. (2021a) designed and determined the parameters for the digging shovel, which was combined with a front soil crushing device, and performed an Engineering Discrete Element Method (EDEM) analysis software simulation for the potato harvester operation. Wang *et al*. (2021b) designed a second-order shovel with a curved transition surface and studied its kinematics. Wang *et al*. (2006) conducted theoretical and practical experiments to determine the design parameters of the digging shovel. Li *et al*. (2013) improved the existing integral flat digging shovel and designed a novel fixed-blade separable biomimetic digging shovel.

Guo *et al*. (2018) experimented with a convex surface shovel design, which reduced the digging resistance of the potato harvester while enhancing its soil crushing capacity. Jia *et al*. (2023) analyzed the application of biomimetic technology in the design of a potato harvester digging shovel, providing an overview of the biomimetic drag reduction digging technology and a reference basis for digging shovel design. Lv *et al*. (2019) designed a second-order convex surface digging shovel to address soil clogging and potato damage during the harvester operation. They conducted a finite element analysis and experimental verification to demonstrate the effectiveness of this design in resolving soil clogging and potato damage problems. Zhao *et al*. (2024) compared the working process and force conditions of potato harvester digging shovels, laying the foundation for optimizing and designing harvester digging components.

Although previous studies focused on the analysis of potato harvester digging shovels, none examined the impact of the inclination angle between the curved shovel surface. This study used the finite element software ABAQUS to create a simulation model of the shovel's contact with the soil, taking into account the face inclination angles α_1 and α_3 and other parameters. The study analyzed the impact of different surface inclination angle α_2 values on the soil crushing capacity of the shovel. This study provides a solid foundation for determining and optimizing the surface inclination angle for potato harvester digging shovels.

MATERIALS AND METHODS

Digging shovel structure

Based on their assembly form, digging shovels can be classified as fixed, driven, or a combination. The fixed digging shovel is directly or indirectly connected to the frame and works in line with the movement of the digging device. It exhibits good stability, is less prone to wear, and effectively reduces the occurrence of potato spillage (Li *et al*., 2021). In hilly regions, potato harvesters commonly use fixed multi-blade shovels during harvesting. Therefore, in this study, the fixed type, three-small-blade shovel structure was used. The design features multiple segments (Figure 1A), which

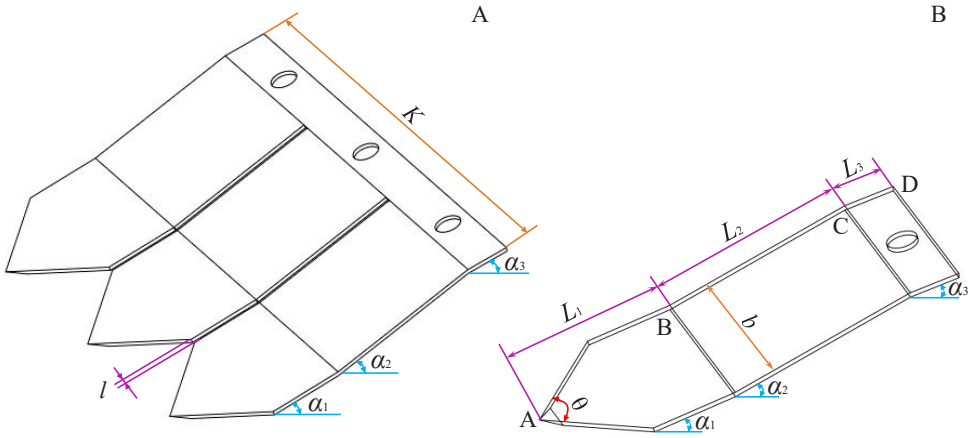

Figure 1. Structure diagram of the digging shovel. A: overall structure; B: single-blade structure diagram. α_1: shovel face inclination angle in segment AB (°); α_2: shovel face inclination angle in segment BC (°); α_3: shovel face inclination angle in segment CD (°); L_1: shovel surface length in segment AB (mm); L_2: shovel surface length in segment BC (mm); L_3: shovel surface length in segment CD (mm); b: single shovel operation working width (mm); θ: shovel blade opening angle (°); l: shovel gap (mm); *K*: effective total width of the digging shovel (mm).

optimize soil penetration, soil crushing, and loosening capabilities of the shovel, while also reducing the occurrence of soil clogging during potato harvesting. The digging shovel adopts an overall symmetric design to ensure uniform force distribution and prevent localized damage due to stress concentration (Figure 1B).

Main parameters of the digging shovel

The digging speed of the potato harvester refers to its forward speed. In this study, the digging shovel needs to adapt to small fields in hilly regions, where tractors with 50–70 horsepower are the most prevalent. Therefore, the maximum operating speed of the tractor is set to v_0 = 1.2 m s^{-1} (Cao *et al*., 2023).

Appropriate digging shovel soil entry parameters are more favorable for excavating the potato-soil mixture and conveying it to the potato separation mechanism. Combined with the actual soil and operating conditions in hilly areas, a mechanical model is established to analyze the forces acting on the digging shovel after entering the soil (Wei *et al*., 2023). In the model, β is the blade opening angle (°); P is the resistance force on the blade (N); F_Z is the frictional force between the potato-soil mixture and the blade (N); R_0 is the force perpendicular to the blade (N); G is the gravity force of the potato-soil mixture (N); F_p is the force required to lift the excavated material along the movement of the digging shovel (N); F_n is the support force of the digging shovel on the potato-soil mixture (N); F_f is the frictional force of the digging shovel on the potato-

soil mixture (N); h_1 is the depth of entry into the soil for segment AB (mm); h_2 is the depth of entry into the soil for segment BC (mm); and h is the total depth of entry into the soil for the digging shovel (mm) (Figure 2).

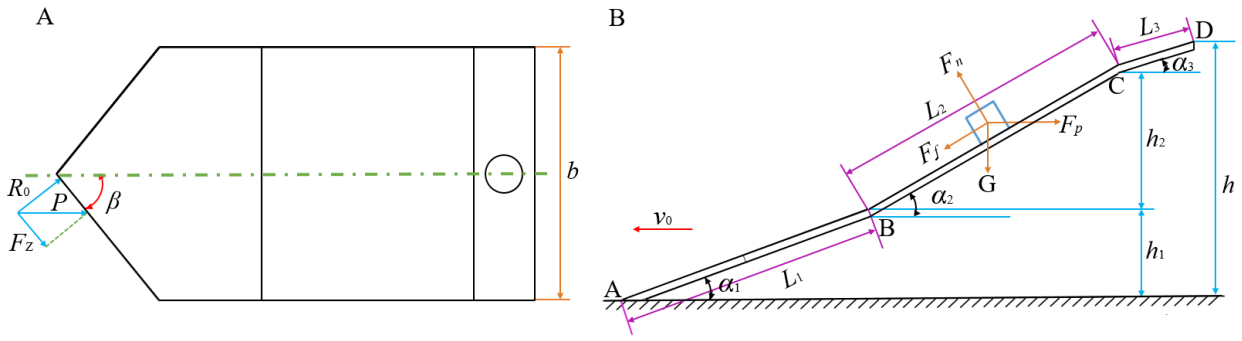

Figure 2. Force analysis parameter diagram of the designed digging shovel. A: Upper view of the shovel; B: lateral view of the shovel.

Design of the blade opening angle for the digging shovel

The optimization of the blade opening angle is aimed at reducing the sliding and cutting resistance between weeds and stems and the digging shovel. A reasonable blade opening angle not only reduces the forward resistance of the shovel but also facilitates the smooth conveyance of the potato-soil mixture to the potato separation mechanism. Moreover, the blade opening angle must be designed to allow both stems and weeds to slide off the blade to prevent clogging (Li *et al*., 2023). The blade opening angle of the digging shovel should satisfy the following equation:

$$F_z < Psin\ (90° - \beta)$$

The friction coefficients for heavy clay and clay with steel are reported to be 0.4–0.9 (Han *et al*., 2024). This study selected the maximum friction coefficient of 0.9. Moreover, the typical blade opening angle for digging shovels is between 44 and 52 °. To meet the design requirements of this study, a blade opening angle β = 50 ° was chosen. Therefore, the blade opening angle θ is equal to 100 ° (Figure 2).

Design of the blade width for the digging shovel

The effective total width K of the digging shovel is mainly related to the underground distribution of potato tubers, row spacing, plant spacing, growth conditions, and deviations in the harvester's travel path (Zhang *et al*., 2021). To ensure that the entire mixture within the potato ridge is excavated, the effective working width of the

digging device should be slightly larger than the ridge bottom width. The working width of the shovel can be determined through the following equation:

$$K = M + e + 3\sigma + 2c$$

where M is the average row spacing (mm), e is the average distribution width of potatoes, (200–250 mm), σ is the composite standard deviation (mm), and c is the machine travel deviation (50–80 mm). The composite standard deviation is calculated as:

$$\sigma = \sqrt{\sigma_M^2 + \sigma_b^2}$$

where σ_M is the standard deviation of row spacing (mm), and σ_b is the standard deviation of potato tuber distribution width (mm).

In this study, M = 300 mm, e = 200 mm, σ_M = 60 mm, σ_b = 60 mm, and c = 50 mm, considering the agricultural requirements of a maximum ridge bottom width of 800 mm and an effective total width K = 834 mm. Since the digging shovel in this study has a fixed three-small-blade structure, the following formula is used:

$$b = \frac{K - 2l}{d}$$

where d is the number of blades in a single shovel body (d = 3), and l is the shovel gap (l = 12 mm).

Design of the digging shovel blade length

In hilly areas, potato tubers are typically distributed below the surface by 150–200 mm (Niu *et al*., 2022). To meet potato growth conditions and ensure a clean harvest, the range for the total depth of entry into the soil for the digging shovel is set to 150–220 mm. Due to variations in the shovel face inclination angle and soil properties, the digging depth has an impact on the traction resistance of the shovel. However, considering that there is a connecting plate installed beneath the digging shovel, and that this connecting plate can also alter the digging depth and is positioned below the ridge top, the actual depth of entry into the soil is approximately 170 mm. Therefore, considering these conditions, the parameter values for this study were h = 170 mm, h_1 = 59 mm, and h_2 = 96 mm.

The shovel length is determined by the following formula:

$$L = \frac{h}{\sin\alpha} \quad (1)$$

Analysis of the shovel face inclination angle

The magnitude of the shovel face inclination angle (α) affects soil penetration and soil crushing performance, digging resistance, and the height of the material lifted by the shovel. A smaller angle reduces the friction between the digging shovel and the potato-soil mixture; however, if the angle is too small, the overall length of the shovel will increase (Wei and Wang, 2024). Therefore, the shovel face inclination angle should satisfy the following equations:

$$F_p cos\alpha - F_f - Gsin\alpha \geq 0 \quad (2)$$

$$F_n - Gcos\alpha - F_p sin\alpha = 0 \quad (3)$$

$$F_f = \mu_1 F_n$$

where in:

$$\mu_1 = tan\phi_1$$

where μ_1 is the friction coefficient between the soil and the digging shovel, and ϕ_1 is the friction angle between the soil and the digging shovel (°).

By simultaneously considering equations (2) and (3), it can be obtained:

$$\alpha \leq arctan\frac{F_p - \mu_1 G}{G + \mu_1 F_p} \quad (4)$$

According to equation (4), a smaller shovel face inclination angle implies better soil penetration performance and lower digging resistance, but poorer soil crushing performance. Correspondingly, a larger angle results in better soil crushing but poorer soil penetration performance with higher digging resistance.

Curved shovels take into account various factors. The front blade section AB segment has a smaller shovel face inclination angle α_1 to improve soil penetration. A larger α_1 is beneficial for ensuring the lifting height and soil crushing requirements. The middle blade section BC segment has an increased shovel face inclination angle α_2 to enhance soil crushing while shortening the length of the digging shovel. The rear stone guard section CD segment reduces the shovel face inclination angle α_3 to promote the loosening of soil subjected to compression (Wang *et al*., 2023). Referring to industry standards for potato harvesters, it is found that α_1 is generally between 10–15 °, α_2 between 16–24 °, and α_3 between 12–15 °. Therefore, considering its soil crushing performance, this study designed the shovel face inclination angle for the AB segment α_1 = 15 ° and for the CD segment α_3 = 13 °.

From equation (1), the following parameters were defined:

Length of the AB segment shovel face:

$$L_1 = \frac{h_1}{sin\alpha_1} = 228\ mm$$

Length of the CD segment shovel face:

$$L_3 = \frac{h - (h_1 + h_2)}{sin\alpha_3} = 67\ mm$$

Maximum shovel face length of the digging shovel:

$$L_{max} = \frac{h}{sin\alpha_1} = 656\ mm$$

The length of the BC segment shovel face is related to the shovel face inclination angle α_2, and therefore, the BC segment shovel face length is defined as:

$$L_2 = \frac{h_2}{sin\alpha_2}$$

When α_2 is 16–17 ° (Table 1), the total length of the digging shovel is too close to the maximum shovel face length, differing only by 13 and 32 mm, resulting in an excessively long digging stroke and a higher likelihood of causing soil blockage. Therefore, a simulation analysis is conducted with α_2 ranging from 18 to 24 °.

Table 1. Data for BC segment shovel face length.

α_2 (°)	16	17	18	19	20	21	22	23	24
L_2 (mm)	348	329	311	295	281	268	256	246	236

α_2: shovel face inclination angles; L_2: shovel surface length in segment BC.

Establishment of the finite element simulation model

The resistance encountered by the digging shovel during the excavation process mainly arises from soil compression and friction. Therefore, it is necessary to analyze the digging conditions of the shovel in the soil.

Model data

Seven data sets are studied, with α_2 values set to 18, 19, 20, 21, 22, 23, and 24 °. In this model, the digging shovel thickness is 6 mm, the AB segment shovel face length L_1 = 228 mm, the BC segment shovel face length as previously shown (Table 1), the CD

segment shovel face length L_3 = 67 mm, and the other parameters remain consistent with the earlier settings, but scaled down by 0.25 times. The soil model was established based on the Saint Venant's Principle (Knops, 2017), with soil dimensions of 200 mm in length, 140 mm in width, and 80 mm in height (Figure 3).

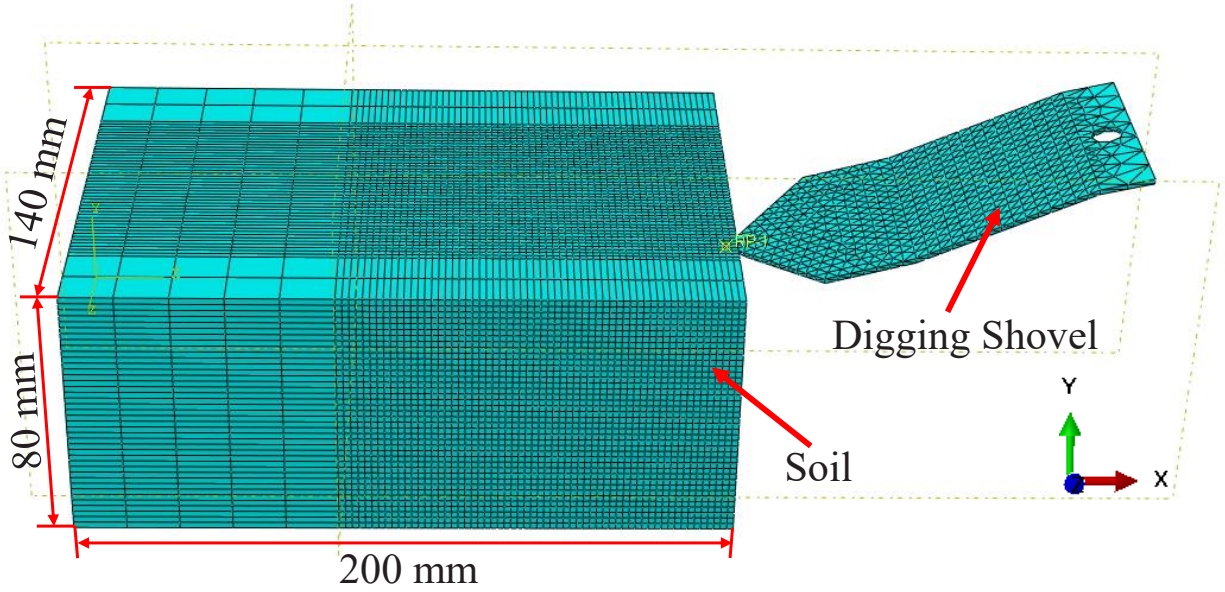

Figure 3. Grid division for the contact model between a single blade of the digging shovel and the soil.

Calculation parameters

The model consists of two parts: the digging shovel and the soil. Mn45 was selected as the material for the digging shovel, with a mass density ρ = 7.85e-9 Mg mm^{-3}, Young's modulus E = 2.09e5 MPa, and Poisson's ratio μ = 0.269. The soil, modeled as clay (Wang *et al*., 2015), has a mass density ρ = 1.8e-9 Mg mm^{-3}, Young's modulus E = 10 MPa, and Poisson's ratio μ = 0.3. Using the Mohr-Coulomb plasticity, the friction angle is 15 °, and the cohesion yield stress is 0.05 MPa. Each component is treated as a homogeneous material.

The overall analysis utilizes dynamic displays, with digging shovel grids employing C3D4 elements and an approximate global size of 4 mm, locally thickened to 10 mm. An explicit linear analysis is applied. Soil grids use C3D8R elements with an approximate global size of 1.5 mm locally thickened to 15 mm. To better simulate the soil fragmentation state, the Smoothed Particle Hydrodynamics (SPH) method is employed (Xu and Deng, 2016), transforming the grid into particles when the stress reaches 0.02 MPa (Figure 3). Fixed constraints are applied to the bottom and sides of the soil, with an 85 mm displacement imposed on the digging shovel in the -X

direction. The model employs general contact, with a friction coefficient of 0.9 between the digging shovel and the soil, and the digging shovel is constrained as a rigid body.

Mesh irrelevance analysis

To validate mesh independence (Figure 4), the simulation model shows how maximum stress and computation time change with mesh size from 4 to 1 mm. When the mesh size is reduced from 4 to 2 mm, the maximum stress initially increases, most likely due to coarser meshes failing to capture stress concentrations and thus underestimating the

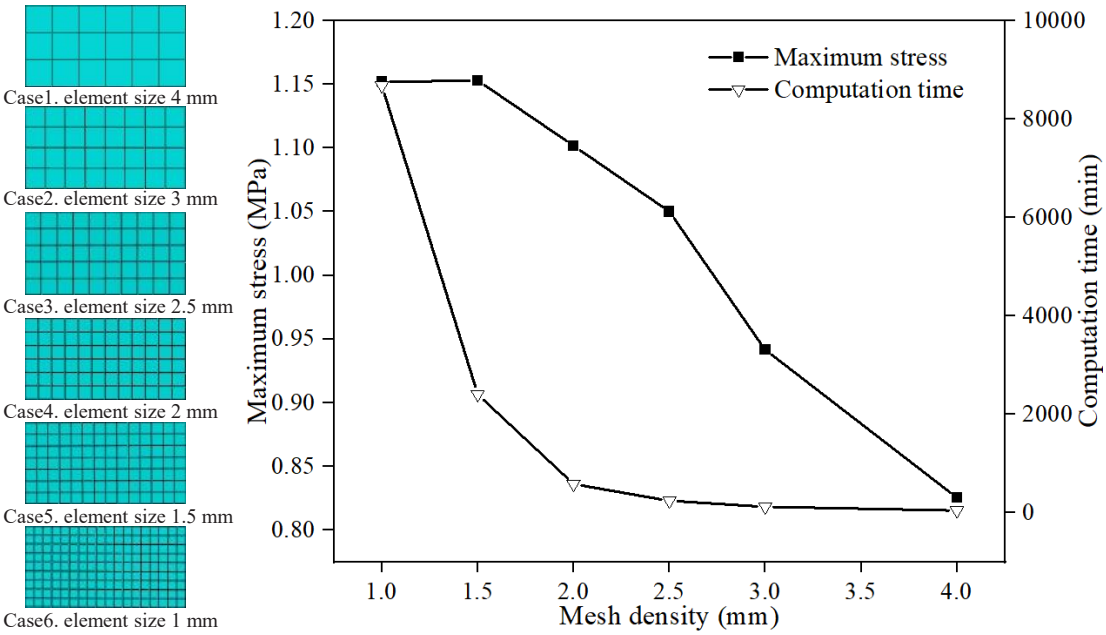

Figure 4. Mesh irrelevance analysis.

stress. However, when the mesh size reaches 1.5 mm, the stress levels drop, indicating that there is enough refinement to represent stress accurately. Reducing the mesh to 1 mm produces a stress difference of 0.001 MPa, demonstrating mesh independence. This stabilization indicates that a 1.5 mm mesh is ideal for balancing accuracy and computational efficiency. Furthermore, the computation time, indicated by the red line, increases dramatically as mesh sizes decrease, particularly below 2 mm, emphasizing the direct relationship between finer meshes and higher computational costs. Choosing a 1.5 mm mesh size is thus ideal for ensuring model accuracy while efficiently managing computation time, making it a practical choice for engineering applications that require precision without excessive computational expenditure. This balance is critical for ensuring the simulation's economic and practical viability, as well as providing a solid foundation for future design optimization.

Plastic Equivalent Strain

This Plastic Equivalent Strain (PEEQ) describes plastic deformation of a material. In the engineering context of excavating soil, the magnitude of the plastic deformation may have different effects on engineering design and execution (Bao *et al*., 2021). Therefore, PEEQ can reflect the deformation of the soil to a certain extent. The greater the soil deformation, the more effective the crushing.

Mechanical Specific Energy

The forward resistance and energy consumption of the digging shovel are the basic characteristics of the soil crushing process (Niu *et al*., 2023). Forward resistance is indicative of the difficulty of breaking ground. The lower the forward resistance, the easier it is for the soil to break and the less energy is consumed. Therefore, this work makes use of the Mechanical Specific Energy (*MSE*) to describe the energy consumed per unit volume of soil crushing to quantitatively represent the crushing efficiency of soil. It provides an important indicator for calculating the soil fragmentation efficiency. When the digging shovel advances horizontally for a distance *r*, the work done on the soil is $F_h r$. If the crushing volume is considered as the volume of the shovel, which can be expressed as the product of its width, the average breaking force, and the breaking stroke, then the *MSE* can be expressed as:

$$MSE = \frac{W}{V_{cut}} = \frac{F_h r}{S_p r} = \frac{F_h r}{bhr} = \frac{F_h}{bh}$$

where *MSE* is the energy consumed per unit volume of soil fragmentation (mJ mm^{-3}), *W* is the energy to break the soil (mJ), V_{cut} is the fragmented volume (mm^3), F_h is the average soil-breaking force (N), S_p is the projection of the fractured area (mm^2), and *r* is the soil-breaking travel distance (mm).

All Field Variables Display

This work assumes an All Field Variables Display (*ALLFD*) is used to output the information of all field variables, including the energy term, combined with the soil simulation model. The maximum variables are extracted under different shovel face inclination angle α_2 values to observe the energy consumed in the process of soil crushing (Namdar and Dong, 2019).

RESULTS AND DISCUSSION

Simulation results analysis

According to Zou *et al*. (2020), the breaking force provides insights into the digging shovel's performance during excavation, with observations made at a shovel face inclination angle α_2 = 19 ° and a specified blade width of 270 mm (Figure 5). The

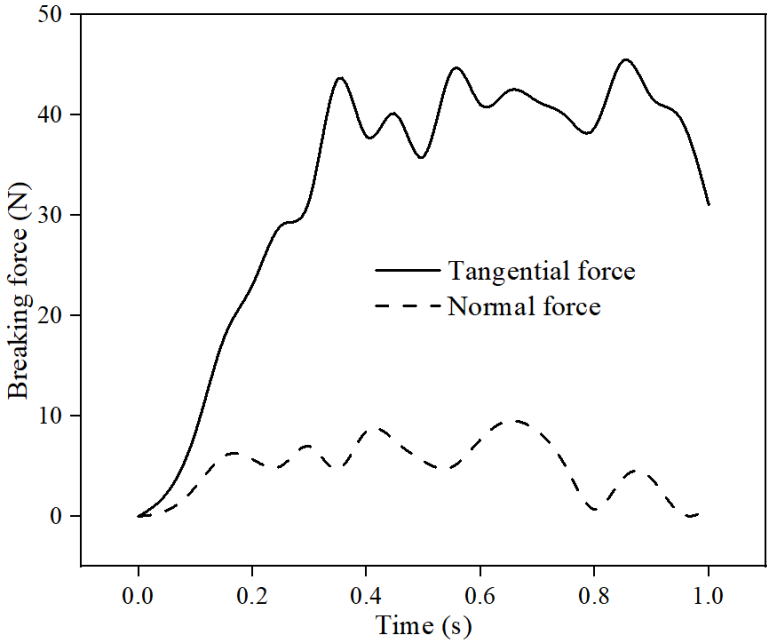

Figure 5. Breaking forces versus time.

positive tangential force indicates resistance against the digging direction, suggesting that the excavator experiences a reactionary force opposing its motion—a typical response when a shovel blade cuts into the soil, encountering resistance from the soil's texture and compactness.

The described positive normal force indicates that the force exerted by the shovel on the soil is perpendicular and directed inward, reflecting the impact of the shovel pushing against the soil during excavation. This force is crucial for effectively dislodging the soil and is indicative of the shovel's penetration power. The rapid increase in breaking force upon contact with the soil, followed by sharp fluctuations, mirrors the dynamic interaction between the shovel and varying soil conditions. These fluctuations could be attributed to different soil densities, moisture levels, or embedded rocks, which intermittently alter the resistance faced by the shovel blade. Overall, this provides a practical understanding of how effectively the shovel can penetrate and maneuver through different types of soil.

Impact of the shovel face inclination angle α_2 on soil stress

The ability to break up soil is an important factor in determining the performance of a digging shovel. Soil stress leads to deformations in the soil mass. Excessive stress in the soil can result in the degradation of its strength (Zhao *et al*., 2016). As a result, soil stress can be used to assess the digging shovel's soil-breaking capability, as demonstrated by a local magnification of the soil fragmentation stress contour plot and the soil stress contour plot (Figure 6).

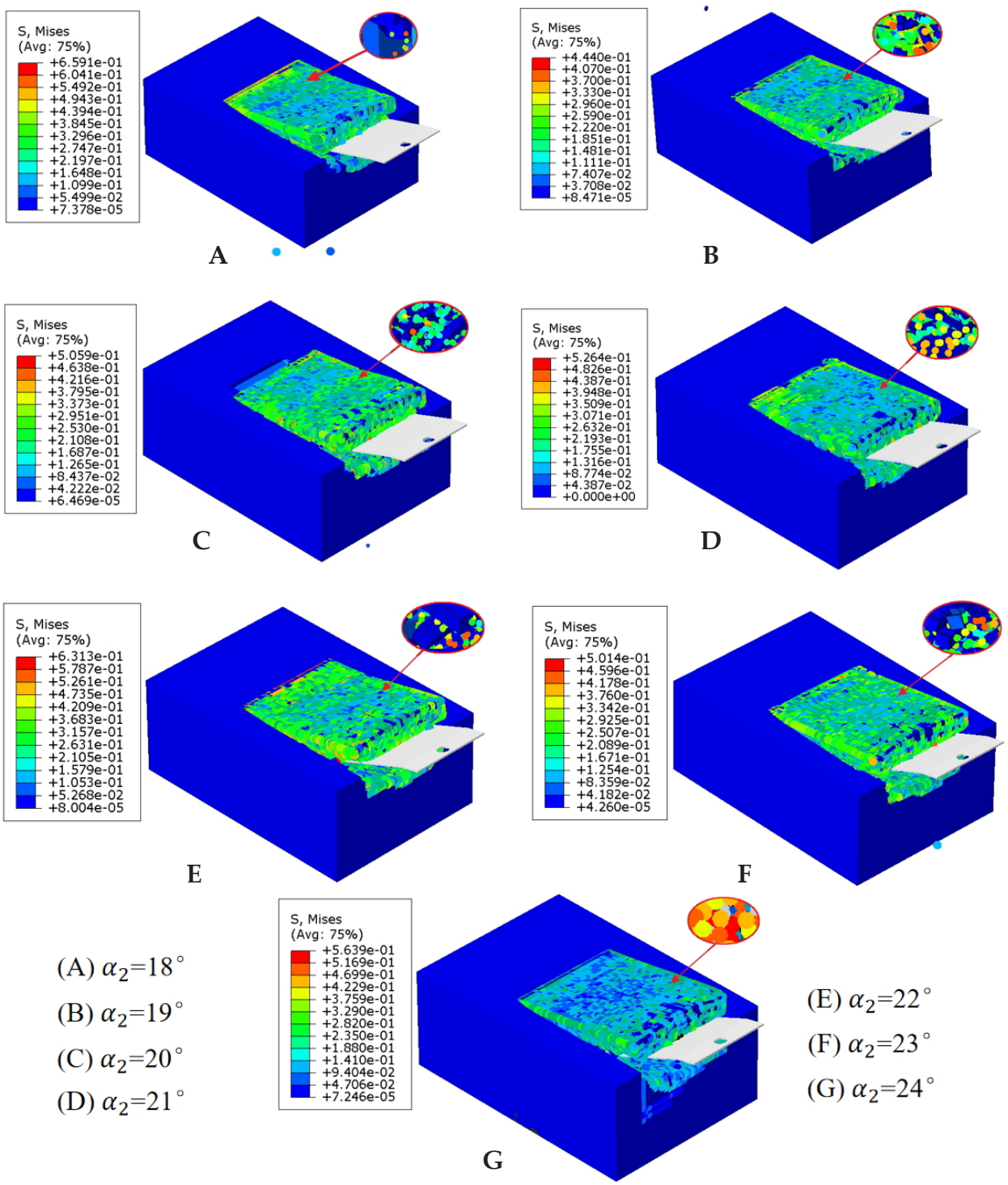

Figure 6. Soil stress contour plot at different shovel face inclination angle α_2 values.

The fragmentation of the soil is related to the inclination angle α_2 of the shovel face. This study extracts the maximum stress of the soil above the BC segment of the shovel face to observe soil fragmentation (Figure 7). When α_2 = 18 °, the soil stress is minimal (0.2 MPa). When α_2 = 19 °, the soil stress reaches 0.37 MPa, showing an increase of 0.17 MPa. When α_2 = 24 °, the soil stress increases significantly to 0.564 MPa, an increase of 0.364 MPa when compared to α_2 = 18 °. Therefore, increasing the inclination angle α_2 of the shovel face leads to increased soil stress and stronger soil crushing ability. However, if α_2 is too large, it may cause the soil to turn back, and the potato mixture cannot be transported to the potato separator completely. Therefore, considering the influence of soil crushing ability, the digging shovel with the lowest soil stress and α_2 = 18 ° is excluded.

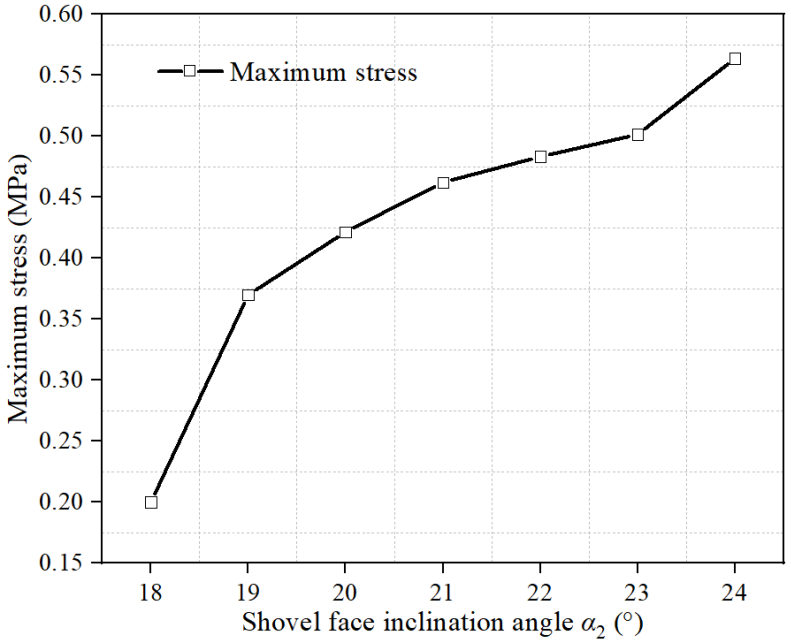

Figure 7. Maximum soil stress above the shovel surface length in segment BC (L_2).

Effect of shovel face inclination angle α_2 on Soil Plastic Equivalent Strain

When the shovel face inclination angle α_2 = 19–22 °, as opposed to α_2 = 18 ° and α_2 = 23–24 °, the red soil particle area gradually increases and is mostly concentrated between the shovel surfaces of the BC section (Figure 8).

The relationship between the maximum Soil Plastic Equivalent Strain (PEEQ) value and the shovel face inclination angle shows that when α_2 = 20 °, the PEEQ and soil deformation are the largest and the crushing ability of the soil is the best (Figure 9A). When α_2 = 19 ° and α_2 = 21–22 °, PEEQ values are the closest, and the difference between them and the PEEQ maximum at α_2 = 20 ° is small. When α_2 = 18 ° or between 23 and

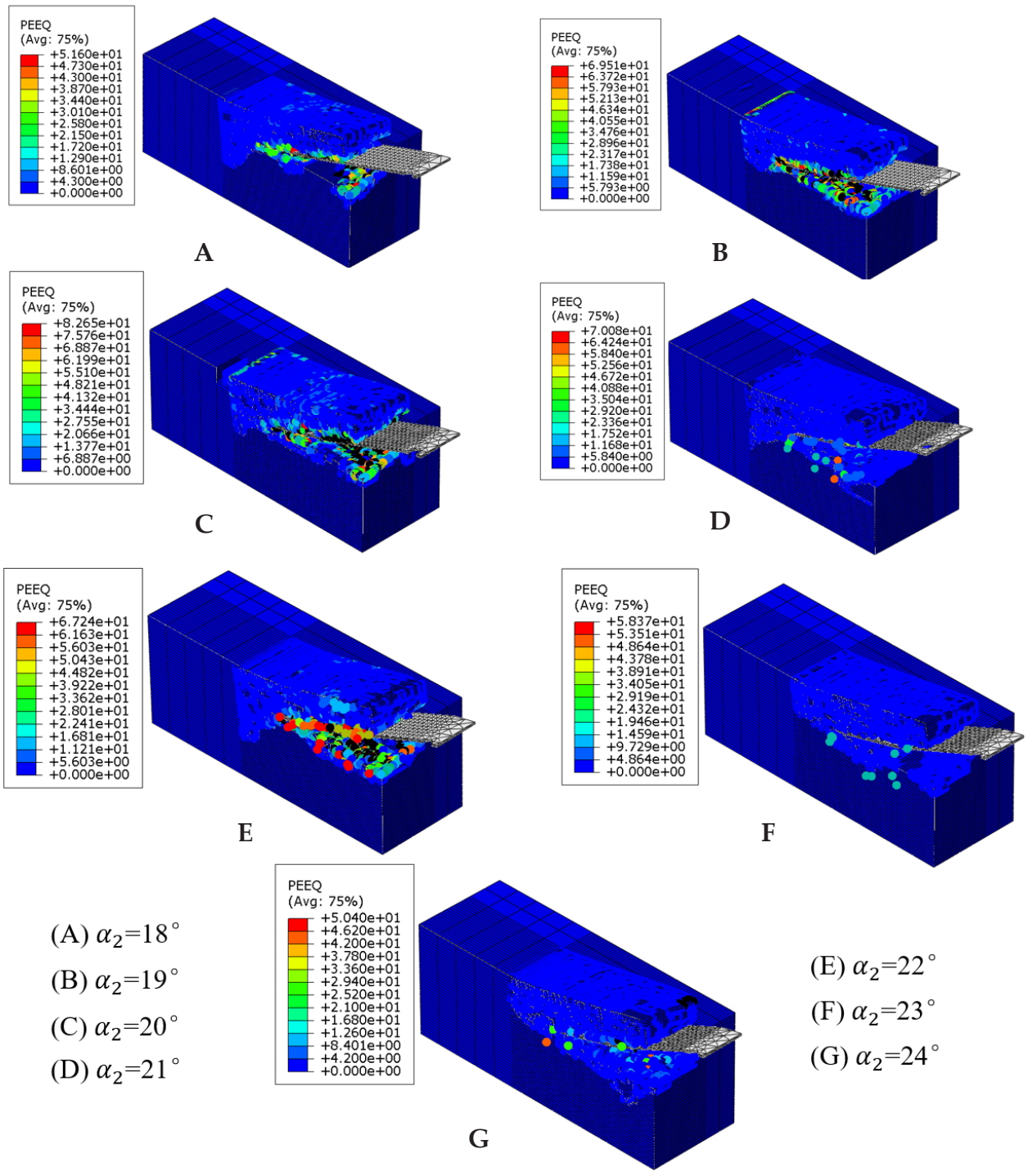

Figure 8. Soil Plastic Equivalent Strain (PEEQ) contour plots at different shovel face inclination angle α_2 values.

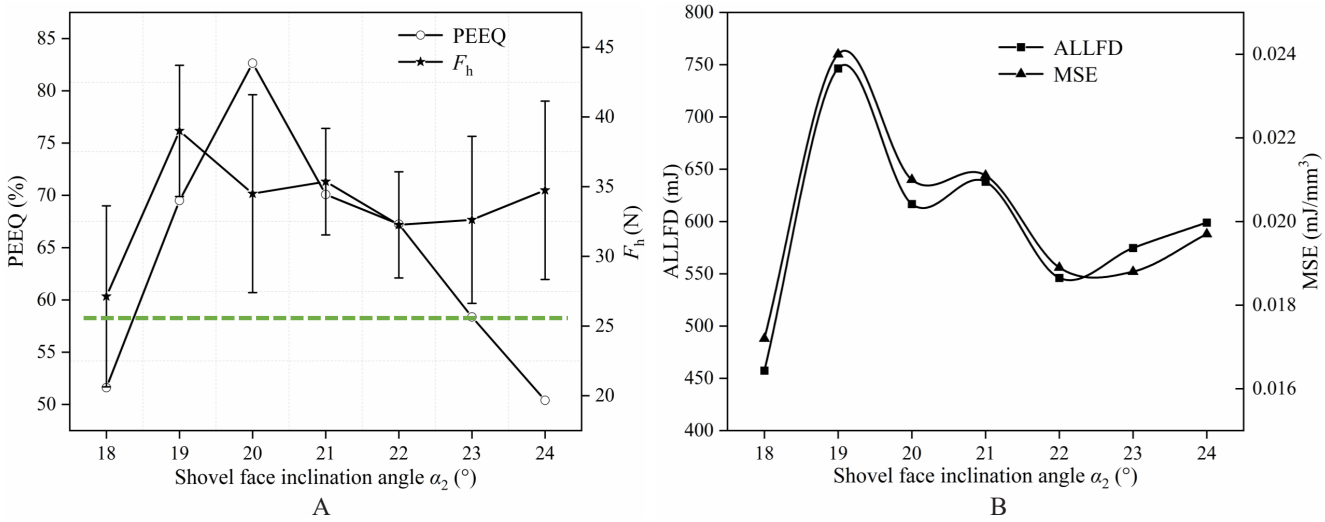

Figure 9. A: Soil Plastic Equivalent Strain (PEEQ) values at different shovel face inclination angle α_2 values and Mean ground breaking force and mean square error. B: Mechanical Specific Energy (*MSE*) at different angles and maximum All Field Variables Display (*ALLFD*) values.

24 °, the strain variable ranges from 50.04 to 58.37 %, which is significantly different from the PEEQ values at other angles. The maximum PEEQ value at 20 ° has a 32.25 % difference compared to the PEEQ values at α_2 = 18 ° and α_2 = 23–24 °. This indicates that soil deformation is smaller at these specific angles. Therefore, considering the influence of soil deformation on the ability to break soil, the digging shovel with small soil PEEQ and shovel face inclination angles α_2 = 18 ° and α_2 = 23–24 ° is excluded.

Effect of shovel face inclination angle α_2 on Mechanical Specific Energy

The average breaking force F_h is a key parameter for evaluating the soil-breaking effectiveness of the shovel blade at different shovel face inclination angles α_2 (Figure 9A). Through simulation analysis at various angles, particular attention was given to the changes in F_h to identify the optimal soil-breaking angle. At an inclination of α_2 = 18 °, the initial F_h value is 27.13 N, and it sharply increases to 39 N at α_2 = 19 °, indicating that the tangential force exerted by the shovel blade on the soil has reached its peak. As the angle increases further, F_h slightly decreases to 34.5 N at α_2 = 20 ° and remains steady at 35.36 N at α_2 = 21 °. Subsequently, at α_2 = 22 ° and α_2 = 23 °, F_h shows a declining trend. This suggests that although the breaking force is highest at α_2 = 19 °, the interaction efficiency between the shovel blade and the soil decreases at larger angles. The optimal soil-breaking angle is around α_2 = 19 °, which is crucial for maintaining effective soil breaking and reducing energy consumption.

The Mechanical Specific Energy (*MSE*) is a critical parameter for evaluating soil-breaking efficiency during excavation (Figure 9B). *MSE* is lowest at α_2 = 18 °. However,

when α_2 = 19 °, *MSE* increases sharply, reaches its peak, and then gradually decreases. When α_2 is between 20 and 21 °, *MSE* remains relatively stable and begins to gradually decline at α_2 = 21 °. During the excavation process, the larger the *MSE*, the more energy is consumed per unit volume of soil breaking, and the greater the work done; therefore, a smaller *MSE* is preferable. Considering energy consumption, the shovel with the highest *MSE* at α_2 = 19 ° is excluded.

Effect of shovel inclination α_2 on All Field Variables Display

When the shovel face inclination angle α_2 = 18 °, the All Field Variables Display (*ALLFD*) value is lower, at 457.39 mJ (Figure 9B). However, when α_2 = 19 °, *ALLFD* increases sharply, and then decreases after reaching the highest peak. When α_2 is between 21 and 24 °, the *ALLFD* decreases, reaching its minimum at α_2 = 22 ° and gradually tending to stabilize. The larger the *ALLFD* value, the more energy is consumed during the excavation process; therefore, the smaller the *ALLFD*, the better. Therefore, considering the magnitude of energy, digging shovels with maximum *ALLFD* and a shovel face inclination angle α_2 = 19 ° are excluded.

CONCLUSIONS

This study identifies that excessively large shovel face inclination angles (α_2 = 23–24 °) result in inadequate soil deformation, making soil crushing less effective. Small inclination angles (α_2 = 16–17 °) lead to an excessive shovel length, reducing operational efficiency. At α_2 = 18 °, the stress exerted is too small, leading to ineffective soil crushing, and at α_2 = 19 °, the energy consumption is too high, making the design less energy-efficient. When α_2 exceeds 22 °, the soil turning phenomenon increases significantly. Soil rollback is most noticeable when α_2 is greater than 24 °. Therefore, the optimal shovel face inclination angle α_2 should be between 20 and 22 °, with fixed angles α_1 = 15 ° and α_3 = 13 °. This range ensures balanced performance by maximizing soil crushing capacity while minimizing energy consumption and avoiding soil flipping back. The findings offer a more efficient and effective solution and contribute valuable insights into the field of agricultural machinery design.

ACKNOWLEDGEMENTS

This work was supported by the Design of a Trailed Potato Harvester in Hilly Terrain (No. XDNY2023-007).

REFERENCES

Bao G, Wang G, Wang B, Hu L, Xu X, Shen H, Ji L. 2021. Study on the drop impact characteristics and impact damage mechanism of sweet potato tubers during harvest. Plos One 16 (8): e0255856. https://doi.org/10.1371/journal.pone.0255856

Cao C, Liu Z, Ding W, Wu M, Zhang X, Qin K. 2023. Design and experiment of Ning-Guo Radix Peucedani bionic digging shovel. Transactions of the Chinese Society for Agricultural Machinery 54 (11): 102–113. https://doi.org/10.6041/j.issn.1000-1298.2023.11.010

Guo X, Feng J, Wang W, Guo S. 2018. Design and research of a second-order convex potato digging shovel. Jiangsu Agricultural Sciences 46 (22): 255–259. https://doi.org/10.15889/j.issn.1002-1302.2018.22.061

Han Z, Bao Y, Xiong Y, Zhang F. 2024. Secondary development of a thermo-elastoplastic constitutive model for saturated clay in ABAQUS. IOP Conference Series: Earth and Environmental Science 861 (7): 072139. https://doi.org/10.1088/1755-1315/861/7/072139

Jia B, Sun W, Zhao Z, Wang H, Zhang H, Liu X, Li H. 2023. Design and field test of a remotely controlled self-propelled potato harvester with manual sorting platform. American Journal of Potato Research 100 (3): 193–209. https://doi.org/10.1007/s12230-023-09909-3

Knops RJ. 2017. New frontiers in Zanaboni's formulation of Saint-Venant's principle. Rendiconti Lincei, Matematicae Applicazioni 28 (2): 255–275. https://doi.org/10.4171/rlm/761

Li J, Gu T, Li X, Wang Z, Hu B, Ma Y. 2023. Analysis and experiment of the bionic drag reduction characteristics of potato digging shovels on clayey black soil conditions. Transactions of the Chinese Society of Agricultural Engineering 39 (20). https://doi.org/10.11975/j.issn.1002-6819.202305034

Li T, Kang J, Sun W, Wang D, Zhang J, Sun B, Wu J. 2013. Design and experiment on 4U-1000 potato harvester. Journal of Gansu Agricultural University 48 (3): 151–155. https://doi.org/10.3969/j.issn.1003-4315.2010.05.026

Li T, Li N, Liu C, Zhu Z, Zhou J, Zhang H. 2021. Development of automatic depth control system employed in potato harvester. Transactions of the Chinese Society for Agricultural Machinery 52 (12): 16–23. https://doi.org/10.6041/j.issn.1000-1298.2021.12.001

Lv J, Wang P, Liu Z, Li Z, Zou F, Yang D. 2019. Design and experiment of potato harvester vine separation device. Transactions of the Chinese Society for Agricultural Machinery 50 (6): 100–109. https://doi.org/10.6041/j.issn.1000-1298.2019.06.011

Namdar A, Dong Y. 2019. Seismic resistance and displacement mechanism of the concrete footing. Shock and Vibration 2019 (1): 5498505. https://doi.org/10.1155/2019/5498505

Niu J, Luo T, Xie J, Cai H, Zhou Z, Chen J, Zhang S. 2022. Simulation and experimental study on drag reduction and anti-adhesion of subsoiler with bionic surface. International Journal of Agricultural and Biological Engineering 15 (4): 57–64. https://doi.org/10.25165/j.ijabe.20221504.6531

Niu S, Li Y, Xie B, Yang Y, Li G, Huang K. 2023. Unit experimental and numerical simulation study on rock breaking mechanism of disc-like hybrid bit. Geoenergy Science and Engineering 228: 212006. https://doi.org/10.1016/j.geoen.2023.212006

Wang D, Bienen B, Nazem M, Tian Y, Zheng J, Pucker T, Randolph M. 2015. Large deformation finite element analyses in geotechnical engineering. Computers and geotechnics 65: 104–114. https://doi.org/10.1016/j.compgeo.2014.12.005

Wang D, Zhang H, Li H. 2006. Design of the mounted potato harvester model 4SM-1. Journal of Agricultural Mechanization Research 8: 122–123. https://doi.org/10.3969/j.issn.1003-188x.2006.08.042

Wang F, Cao Q, Li Y, Pang Y, Xie K, Zhang Z. 2023. Design and trafficability experiment of self-propelled potato harvester in hilly and mountainous areas. Transactions of the Chinese Society for Agricultural Machinery S2: 10–19. https://doi.org/10.6041/j.issn.1000-1298.2023.S2.002

Wang F, Xiong H, Lai Q, Liu Z, Chen K, Lu C. 2021a. Research on the intelligent design system and evaluation method of the digging device of a potato harvester. Transactions of the Chinese Society of Agricultural Machinery 52 (8): 12. https://doi.org/10.6041/j.issn.1000-1298.2021.08.008.

Wang H, Zhang Z, Ibrahim I, Xie K, Wael E, Cao Q. 2021b. Design and experiment of small-sized potato harvester suitable for hilly and mountainous areas. Acta Agricultural Zhejiangensis 4: 724–738. https://doi.org/10.3969/j.issn.1004-1524.2021.04.18

Wei H, Wang D, Lian W, Shao S, Yang X, Huang X. 2013. Development of 4UFD-1400 type potato combine harvester. Transactions of the Chinese Society of Agricultural Engineering 29 (1): 11–17. https://doi.org/10.3969/j.issn.1002-6819.2014.03.002

Wei J, Wang J. 2024. Virtual design and simulation of 4U-1A Potato Harvester. *In* 2009 IEEE 10th International Conference on Computer-Aided Industrial Design & Conceptual Design. Institute of Electrical and Electronics Engineers: Wenzhou, China. https://doi.org/10.1109/caidcd.2009.5375087

Wei Z, Wang X, Li X, Wang F, Li Z, Jin C. 2023. Design and experiment of crawler self-propelled sorting type potato harvester. Transactions of the Chinese Society for Agricultural Machinery 54 (2): 95–106. https://doi.org/10.6041/j.issn.1000-1298.2023.02.009

Wei Z, Wang Y, Su G, Zhang X, Wang X, Cheng X, Jin C. 2024. Research progress on mechanized potato harvesting and impurity removal technology and equipment. Transactions of the Chinese Society of Agricultural Engineering 40 (10). https://doi.org/10.11975/j.issn.1002-6819.202311148

Xu X, Deng X. 2016. An improved weakly compressible SPH method for simulating free surface flows of viscous and viscoelastic fluids. Computer Physics Communications 201: 43–62. https://doi.org/10.1016/j.cpc.2015.12.016

Zhang Y, Qiao C, Wang T, Cao J, Wang P, Shi L. 2021. Drag reduction mechanism of the 3D geometry of foreleg's claw toe of the mole cricket (*Gryllotalpa orientalis*). Transactions of the Chinese Society of Agricultural Engineering 37 (19): 309–315. https://doi.org/10.11975/j.issn.1002-6819.2021.19.0 36

Zhao C, Liu Z, Shi P, Li J, Cai G, Wei C. 2016. Average soil skeleton stress for unsaturated soils and discussion on effective stress. International Journal of Geomechanics 16 (6): D4015006. https://doi.org/10.1061/(asce)gm.1943-5622.0000610

Zhao H, Yu M, Zhang Y, Wei K. 2024. Multi-objective optimization design of a potato digging shovel based on response surface methodology. Computer and Digital Engineering 52 (2): 584–589. https://doi.org/10.3969/j.issn.1672-9722.2024.02.051

Zou J, Han J, Zhang T, Yang W. 2020. Experimental investigation and numerical analyses for red sandstone rock fragmentation. International Journal of Geomechanics 20 (12). https://doi.org/10.1061/(asce)gm.1943-5622.0001869